Effort analysis of the landing gear with possible flow during touchdown

W. Krason, J. Malachowski

***Abstract*—**Dynamic analyses of the landing gear are conducted to provide capabilities to forecast their behavior under hazardous conditions. This kind of investigation with numerical methods implementation is much easier and less expensive than stand tests. The major advantage of the presented numerical method is applicability to landing gear tests with artificially introduced flaws.

***Keywords*—** FE modelling, landing gear, drop test simulation, possible flaw.

I. Introduction

NUMERICAL movement analysis should be examined already at the early stage of the product lifecycle, which is the design process. It means the machine, which motion is to be simulated, has not been manufactured yet. The only way to carry such an examination is to test the digital model imported from the CAD system. In 1990's, about 95% motion simulations had been carried with the real (already manufactured) mechanisms. Results of such an analysis are subjective, because: many elements of the real mechanisms are manufactured imperfect, according to the design documents, it is not possible to measure the movement of real mechanisms with wanted high precision at low costs. Furthermore, if the motion analysis enables engineers to detect serious motion errors: it takes much time to improve the designs, it is very dangerous (for the staff) to deal with such a mechanisms, if they're already available on the market [1,4,8,10,13].

Numerical simulations are helpful in detecting all dangerous mechanisms conditions, what increases the safety and reliability of the maintenance process. The primary purpose of the landing gear units is to absorb the impact energy of the aircraft when it lands and takes off [2,11]. Therefore landing gear design comprises very difficult and responsible unit of overall project. This unit has to sustain appropriate strength to guarantee safety and fatigue life that assures the number of takeoff-lands prescribed in the technical specification. Majority of the fatigue numerical analysis and prediction of the landing gear's lifetime is limited to the linear analysis and the local phenomena appearing around a failure [7,8,15].

The influence of a failure on the complete landing gear system are subject of our consideration. Various 3D models of the landing gear part with failure were defined for the static FE analysis. Complete system of the main landing gear was mapped as the deformable 3D numerical model for dynamic analysis with LS-Dyna code. Experimental and numerical research of transport airplane's landing gear (Fig. 1) are discussed in this paper.

Fig. 1 view of the drop stand and the failure of the top landing gear's leg

II. Problem Formulation

Based on the aviation regulations [4] plan of the experimental tests for main landing gear was worked out. Such laboratory test schedule complied with operation standard expected for the landing gear of military transportation airplane. Chosen experimental test were carried out on the drop stand presented in Fig. 1. Component forces in the landing gear part, accelerations and displacements were recorded during stand tests. Service fracture in the top leg of landing gear was appeared during the fatigue test. This fracture was caused by technological factors (disturbances). View of the face failure in the top landing gear 's leg was presented in Fig. 1.

Manuscript received January 29, 2008; Revised received March 25, 2008 Polish Committee for Scientific Research supported. This support is acknowledged gratefully.

Wieslaw Krason is with the Department of Mechanics and Applied Computer Science of Military University of Technology, Gen. S. Kaliskiego Street 2, 00-908 Warsaw, POLAND (corresponding author to provide phone: +48 22 6839654; fax: +48 22 6839355; e-mail: w.krason@wme.wat.edu.pl).

Jerzy Malachowski is with the Department of Mechanics and Applied Computer Science of Military University of Technology, Gen. S. Kaliskiego Street 2, 00-908 Warsaw, POLAND (corresponding author to provide phone: +48 22 6839683; fax: +48 22 6839355; e-mail: j.malachowski@wme.wat.edu.pl).

Failures of landing gear are significant problem in the aircraft operating and safety of the aviation transport [7,18]. Fatigue fracture occur in the subassemblies of landing gear often [17,18,21]. An identification of such failures is a difficult task of airplanes service and important problem for a safety assurances [7,19]. Reasons of the landing gear failures and various methods of their study are subject of the scientific consideration from many years [2,7,8,15]. The study described in [20] confirm, that service fracture in the landing gear of airplanes can be conditionally divided into three classes: fatigue fracture, wear and tribomating components, and fractures (fatigue and corrosion) caused by technological factors. The third class is the most dangerous because these fractures cannot be predicted beforehand and are not always detected by cyclic inspections and nondestructive test methods. The failure investigated in this paper (see Fig. 1) belongs to the third class of fractures caused by technological factors – disturbances from the welding process.

III. Numerical analysis - theoretical foundations

For the elastic range, the deformation process of metal parts of landing gear (made of the 30HGSNA and the 30HGSA steels) has been described with the stress deviator [4,13,17]:

$$D_\sigma = 2G\,D_\varepsilon \tag{1}$$

whereas the isotropic component of the stress tensor (axiator) is expressed with the following relationship:

$$A_\sigma = 3KA_\varepsilon \tag{2}$$

where: G – modulus of elasticity in shear, K – modulus of volume elasticity, D_ε – strain deviator and A_ε – isotropic component of the strain tensor (axiator).

The process of the material plasticization takes place at the moment of transition from the elastic state to the plastic one. The yield point determines limits of the state of plasticization. The isotropic hardening of the material manifests itself in that the yield stress is independent on the loading technique. The plastic flow area keeps extending with its form preserved. The extension of the area of plastic flow depends on the strain hardening parameter κ [6,13,17]. In the range of plastic strains the yield point is modified, according to [6,13,17]:

$$\sigma_y = \sigma_o + \beta\frac{3}{2}E_p\varepsilon_{eff}^{p} \tag{3}$$

where: β – strain hardening parameter, E_t – tangential modulus, E – Young's modulus for linear range, E_p – linear strain hardening.

In the case under consideration the problem of contact between collaborating parts has been described with the calculation method based on the penalty function [3,6]. This function can be applied to normal displacements in the displacement-based approach; to normal velocities defined in the velocity-based approach; and to normal displacements in the velocity-based approach, the latter being the most often form of application. In the penalty function method the normal contact force is expressed with the following equation:

$$F_{nij} = \zeta u_{nji} H(-u_{nji}) \tag{4}$$

where: $H(\cdot)$ – Heaviside step function, and $\zeta = 1/\kappa$, κ – coefficient of the penalty function.

Conditions of contact are checked on the grounds of $\mathbf{B}u \geq \gamma$, where $\mathbf{B}$ – matrix that describes boundary conditions kinematics, γ - vector of initial gap. In the course of numerical application of this method an imaginary energetic term is added in the form of the penalty function [4,6]: $\pi = 1/2u^T\mathbf{K}u - u^Tf + \kappa[(\mathbf{B}u - \gamma)^T(\mathbf{B}u - \gamma)]$. In terms of physical interpretation of the penalty function parameter, operation thereof should be interpreted as an imaginary elastic element that appears between two nodes in contact. Value of this parameter [4,6] is found on the basis of accuracy of a computing machine, number of unknowns, and the least stiffness of elements in contact at the moment.

In the constructed numerical model of the landing gear account was taken also of the support-wheel-related subassembly, which includes such elements as: the wheel pin, the wheel rim, and the tyre. (Figs 1 and 2). All parts of this subassembly, belt in the tyre excluded, were represented with the flexible hexagonal elements. Four-node membrane elements were used to describe the belt itself. This enabled the non-homogeneous layers (fabric model) of the tyre cord (that are to be found throughout the tyre cross-section) to be identified using the composite-dedicated materials chart [5,6,15]. Based on author's opinion [6] this material is strongly recommended for modelling airbags. In addition to being constitutive model, this model also invokes a special membrane element formulation that is better suited to the large deformations experienced by fabrics. For thin fabrics, buckling can occur with the associated inability of the structure to support compressive stresses.

What was mapped in the model was the tyre inflated with air under the pressure of 0.55 MPa, i.e. pressure in an actual tyre of the transport's wheel. To model this process, the parameter card available in the LS-Dyna system was used. This card is labelled with the following 'name': AIRBAG_SIMPLE_PRESSURE_VOLUME [6]. In this model the airbag is treated as a control volume. The volume is defined as the volume enclosed by a surface. In analysed case the control volume were modelled by shell elements comprising the airbag fabric material. The area of the control surface which surrounds analysed volume is related to the control volume according to Greens's theory based on the following equation [6]:

$$\iiint \phi\frac{\partial\psi}{\partial x}dxdydz = -\iiint \psi\,dxdydz + \oint \phi\psi n_x d\Gamma \tag{5}$$

where two first integrals are related with a closed volume, i.e. *dv=dxdydz*, and the last integral is an integral over the surface enclosing the volume, and n_x is the direction cosine between the surface and normal and the *x* direction. The similar forms can be written for the other two directions. The two arbitrary functions, it means ϕ and ψ, need only be integrated over the volume and surface.

To describe other rubber components of the tyre, such as a tyre tread and tyre sides, a material model of rubber (based on the Mooney-Rivlin theory [6,13,15]) was applied. Based on this theory the large deformation are able to be taken into consideration. In this model the strain energy density function is defined as in terms of the input constants *A*,*B* and *v* as:

$$W(I_1,I_2,I_3)=A(I_1-3)+B(I_2-3)+C\left(\frac{1}{I_3^2}-1\right)+D(I_3-1)^2$$
$$C=0.5A+B \qquad (6)$$
$$D=\frac{A(5\nu-2)+B(11\nu-5)}{2(1-2\nu)}$$

where *v* is Poisson's ratio and $G= 2(A+B)$ is shear modulus of elasticity. The strain invariants are related to the right Cauchy-Green tensor **C** as:

$$I_1=C_{ii},\ I_2=\frac{1}{2}C_{ii}^2-\frac{1}{2}C_{ij}C_{ij},\ I_3=det(C_{ij}) \qquad (7)$$

The principal components of Cauchy stress, σ_i, are presented as follows [6]:

$$J\sigma_i=\lambda_i\frac{\partial W}{\partial\lambda_i} \qquad (8)$$

where for uniform dilatation $\lambda_1=\lambda_1=\lambda_1=\lambda$.

Finally, the second Piola-Kirchoff stress tensor, **S**, is defined by the partial derivative of strain energy *W* with taking into consideration the Green—Lagrange strain tensor **E** [6]:

$$S_{ij}=\frac{\partial W}{\partial E_{ij}}=2\frac{\partial W}{\partial C_{ij}}=2\left(A\frac{\partial I_1}{\partial C_{ij}}+B\frac{\partial I_2}{\partial C_{ij}}+\left(2D(I_3-1)-\frac{2C}{I_3^2}\right)\frac{\partial I_3}{\partial C_{ij}}\right) \qquad (9)$$

From the numerical point of view, the analysed structural domains were described with Lagrangean formulation. For the domain, the governing equation is the conservation of momentum. By expressing equilibrium in the current configuration and based on Finite Elements, the discrete differential equation is presented as follows [6,17]:

$$\underset{\sim}{M}\underset{\sim}{\ddot{u}}=\underset{\sim}{f}^{ext}-\sum_e\int_{V^e}\underset{\sim}{B}^T\underset{\sim}{\sigma}dV \qquad (10)$$

where $\underset{\sim}{\sigma}$ is the tensor representing Cauchy stress in the structure, $\underset{\sim}{M}$ is a mass matrix, $\underset{\sim}{\ddot{u}}$ is the vector of nodal accelerations, $\underset{\sim}{f}^{ext}$ is the vector of external forces, $\underset{\sim}{B}$ is the matrix of shape functions derivatives and V^e describes the element (*e*) volume. An underlying ~ is related to vector, matrix or tensor quantities. At the initial stage of the tests given consideration, numerical tests were performed to simulate the drop test of the structure with associated masses representing reduced mass of transport airplane. Calculations were made using the so-called direct-integration procedure, colloquially called the "explicit integration" [17].

IV. Numerical 3D Complete Models of the Main Aircraft Landing Gear

A geometric model of a complete landing gear shown in Fig. 2 has been used to generate a totally deformable discrete FE model (Figs 3, 4 and 5) to investigate into the dynamics of the landing gear of a transport aircraft.

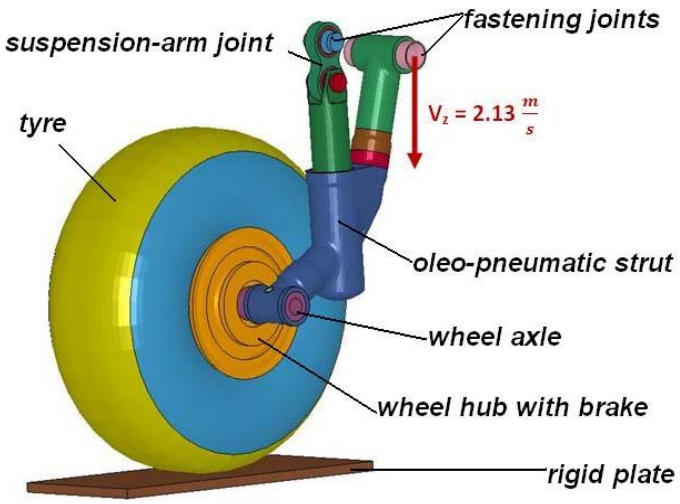

Fig. 2 geometric model of the complete main landing gear

The modelling has been carried out in the MSC.PATRAN environment, the 2005 version, with the LS-Dyna code preferably applied to conduct dynamic analyses. What has been defined for individual solids of the geometric model, which represent particular sections of the landing gear, are the FE meshes, models of materials, and respective types and properties of finite elements that represent the modelled sub-assemblies.

Solid elements of the HEX8 type have been used to model the following structural members of the landing gear: the lower and upper levers of the landing-gear strut, the suspension-arm joint with cup-and-ball joint assemblies – bearing races and pins, the piston rod of the shock absorber with rings and the stem fastening it onto the suspension-arm joint, the shock-absorber's sleeve, the wheel axle with a pin

fastening it to the strut's lever, the landing-gear wheel hub, the brake stator and rotor discs, and the tyre (see Figs 2,3,4 and 5).

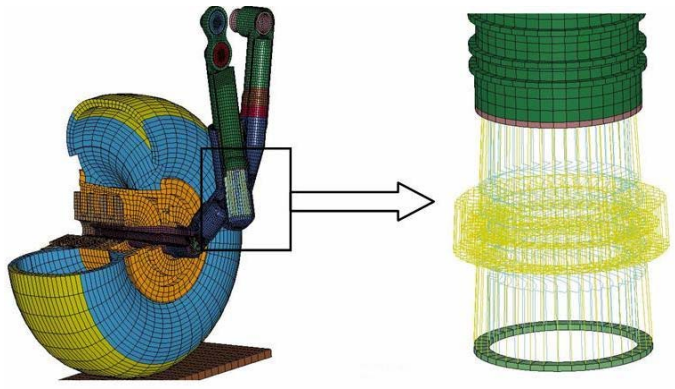

Fig. 3 discrete model with the shock-absorber model included

The model of a complete landing gear comprises 73146 finite elements of the HEX8 type. The complete model of the landing gear with the wheel included comprises 98009 nodes, 2760 surface elements of the QUAD4 type, and 120 MPC elements. Surface elements have been used to map the inner surface of the tyre. The AIRBAG [6] has been defined within the tyre-model interior limited with this surface. The objective thereof is to provide a numerical model with the mapping of the effect of the gas compressed in the wheel. What is simulated in the model is some limited (closed) volume defined with surface elements, the location and orientation of which are checked in each step of calculations. The elastic-and-damping system of the shock absorber has been replaced in the considered discrete model of the landing gear with a set of 40 elements of springs and dampers of linear characteristics [6,12,16,22]. The set of 40 elastic elements and 40 damping elements have been joined directly to the nodes on the edges of additional rigid rings modelled between the cross-section of the bottom of the lower lever of the landing gear and that of the shock-absorber's end face. For each elastic element the same rigidity $K_{n=40}$ = 10.75 *N/mm* has been defined. On the other hand, for each damping element the same value of the viscotic damping $C_{n=40}$ = 2.65 Ns/mm has been defined. Fig. 3 illustrates implementation of the elements in question into a three-dimensional (3D) model.

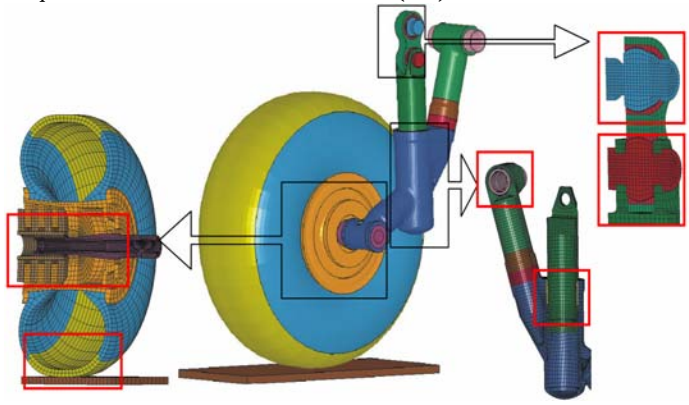

Fig. 4 selected regions of contact, defined in the model of a complete landing gear

In fact, reflected here in the 3D model particular structural members of the landing gear system keep mating to transmit loads through contacting one another. The mapping of the correct mating of the system's members in question requires that appropriate regions of contact are mapped in the numerical model. Twelve couples in contact that include surfaces of some structural members of the landing gear have been defined in the model. These are as follows: the wheel hub and the brake stator – two contact areas (Fig. 4), the wheel axle and the bearing races of the wheel hub – three contact areas, the piston rod of the shock absorber and rings and the cylinder sleeve of the lever – four contact areas, the bearing races and pins of the cup-and-ball joint assemblies – two contact areas, and the upper lever of the strut and the fixing sleeve – one contact area.

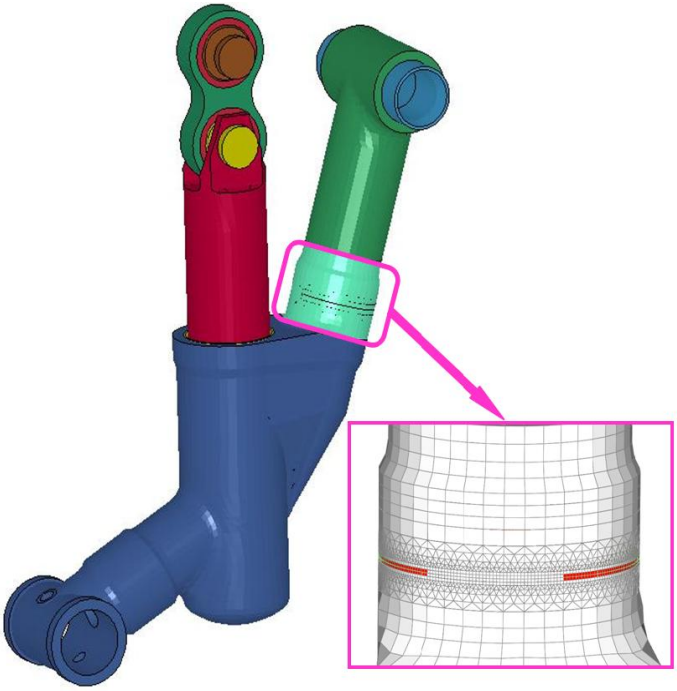

Fig. 5 view of 3D model with the two gaps of fatigue fracture

The 3D model described above (see Figs 2,3 and 4) was developed for dynamic drop test of complete landing gear.

Another version of the numerical landing gear model was built for FE analysis with failure. Details of such model with the two gaps of fatigue fracture were presented in Fig. 5.

V. Dynamic Analysis of the Landing Gear Drop Test

The instance of the landing gear drop from some specific height, i.e. the case given consideration in the paper, was carried out under laboratory conditions on the drop–weight testing machine. This corresponds to the touchdown when an aircraft lands on the tricycle landing gear, i.e. the nose wheel and the main gear, and the loads effected by the

ground/pavement response are distributed on the nose wheel and both landing gear struts.

The objective of the numerical simulation in question was to define the dynamic characteristics of the landing gear, with the vertical-drop test represented (i.e. with no account taken of the forward speed). Numerical analyses were carried out to represent the drop test of the landing gear of an aircraft with the take-off/landing weight of 7500 kg. Numerical simulations of the touchdown were conducted for the parameters that corresponded with those typical of stand tests. They were as follows: m_r = 3325 kg – reduced mass that falls to the landing gear in question, equal to the weight, of all components of the dropped system, V_z = 2.13 m/s – the rate of vertical descent of the aircraft at the moment of the tyre's touching the ground (Fig. 2), V_x = 0 m/s – the landing (horizontal) speed of the aircraft, h = 231 mm – the model-drop height, α = 0 deg – the angle of pitch of a given plane of the aircraft against the ground, P_{am} = 5 MPa – pressure of filling the shock absorber and P_{op} = 0.55 MPa –pressure of filling the tyre.

The FE model of the complete landing gear was applied to define the effort of particular components of the structure during the drop simulation, to examine how the energy of such a system was changing, and deformations that occur in the particular components of the complete aircraft landing gear. It is impossible to record most of these quantities during the tests. What should be emphasized is that the numerically represented test corresponded with the real time interval of the touchdown, i.e. 0.2 s.

Boundary conditions that correspond to those applied in the numerical-test variant under accomplishment were introduced in the landing-gear model. External constraints in the form of fixed pivot bearings were introduced in the nodes that attach the landing gear to the aircraft fuselage structure (i.e. central nodes on side surfaces of the upper pin and the upper-lever sleeve – Fig. 4). What results from numerical tests is a series of data that describe the mating of particular landing-gear structural components in contact areas. It refers to both the kinematics and the dynamics of the structure under consideration. Some selected results of the numerical test showing stress analysis have been shown in Figs 6, 7, 8.

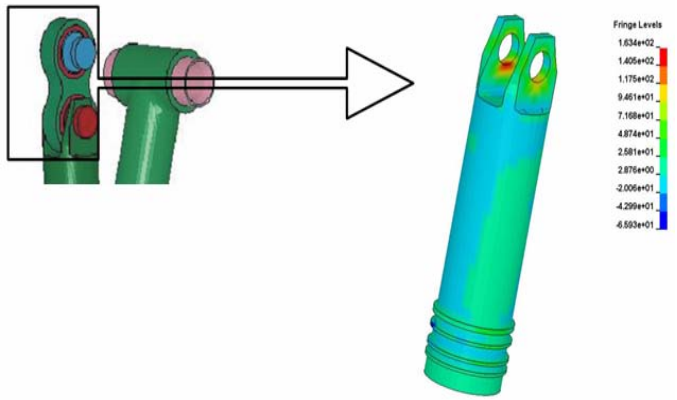

Fig. 6 map of maximum principal stresses in the contact area of the shock-absorber's body (stem) within the node of the pin fastening it to the joint assembly of the landing-gear suspension arm; the data recorded at the touchdown (σ_{max} = 163.4 MPa)

a)

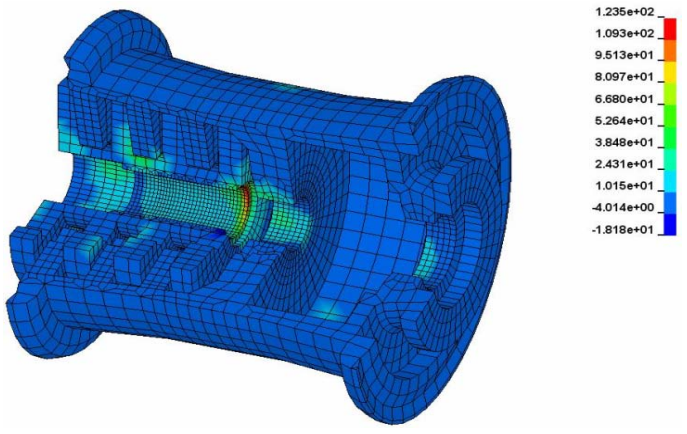

b)

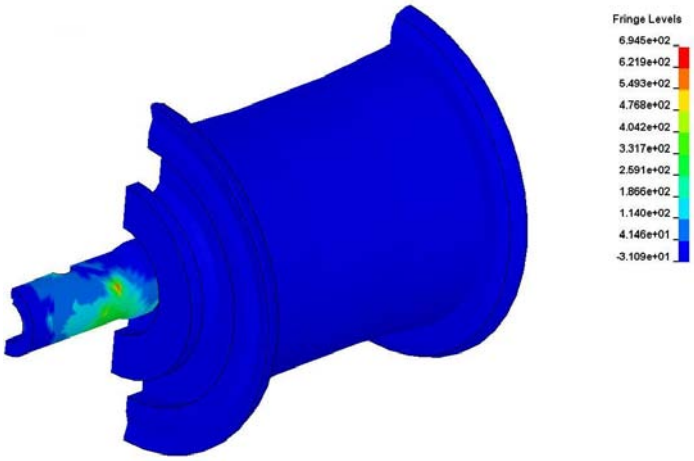

Fig. 7 a) map of maximum principal stresses in the contact area of the main gear's wheel hub and brake stator disc; the data recorded at the touchdown (σ_{max} = 123.5 MPa) and b) the map of maximum principal stresses in the contact area of the main gear's wheel axle and bearing; the data recorded at the touchdown (σ_{max} = 694.5 MPa)

The maximum value of stresses recorded at the touchdown in the contact area of the shock-absorber's member and the suspension-arm joint assembly is σ_{max} = 163.4 MPa. The maximum principal stresses in the contact area of the landing gear's wheel hub and brake stator disc, recorded at the touchdown, reach value of σ_{max} = 123.5 MPa, see Fig. 7. They are located on the edge of the brake stator hole, where the landing-gear's wheel axle is mounted.

a)

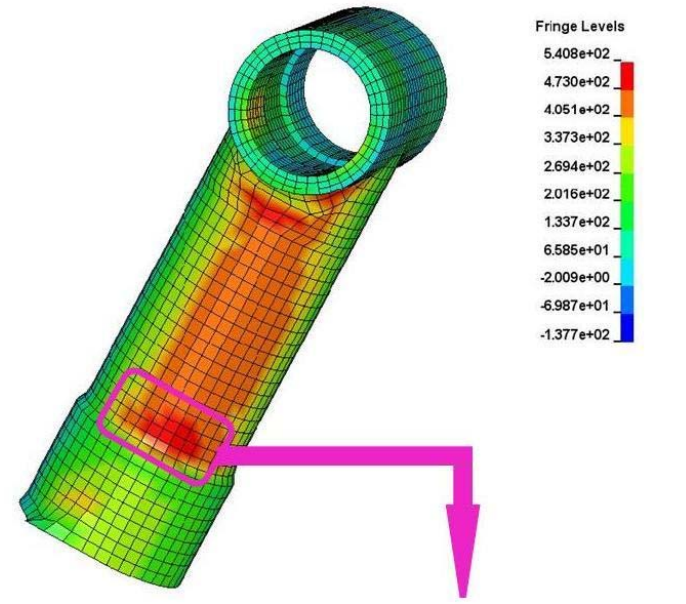

b)

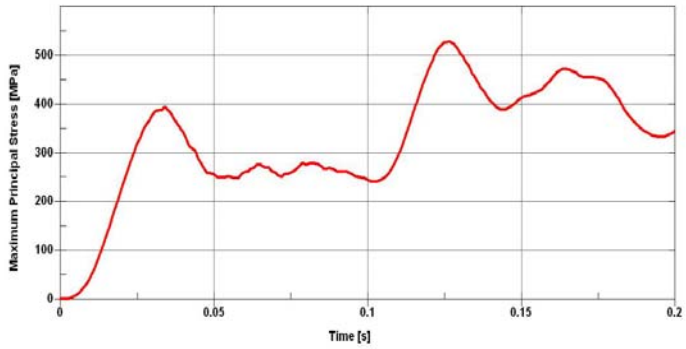

Fig. 8 a) map of maximum principal stresses and how they change within the area of the welded joint that connects the upper and lower levers of the main landing gear;
b) the data recorded at the touchdown
(σ_{max} = 540.8 MPa)

Considerably higher contact stresses can be observed in the contact area of the axle and the inner surface of the bearing of the main gear wheel. Maximum principle stresses within some small area on the wheel axle attain value of approximately 700 MPa.

In the main gear's structure many locations have been observed where local stress concentrations could initiate fatigue cracking (see Fig. 8). However, it should be emphasised that the 3D model in question is an ideal model, with no account taken of any failure at any stage.

Fig. 8 shows the map of maximum principal stresses and the plot of how they change in elements distinguished within the area of the welded joint that connects the upper and the lower levers of the main landing gear. The map of the effort gained from the above-mentioned simulation explicitly confirms that within the area of the welded joint, which connects the upper and lower levers of the examined landing gear, considerable local stress concentrations occur. These observations confirm results of tests conducted on a real object. It has proved that stand tests which consisted in the reproduction of a complete operational cycle have resulted in the landing-gear failure.

What has also been included in the paper are analytical results that illustrate the quality of the numerically representing the landing-gear drop under laboratory conditions. Therefore, changes in the shock-absorber's body displacement against its cylinder and changes in the vertical response recorded on the model of the drop-weight plate have been shown in Figs 9 and 10, respectively.

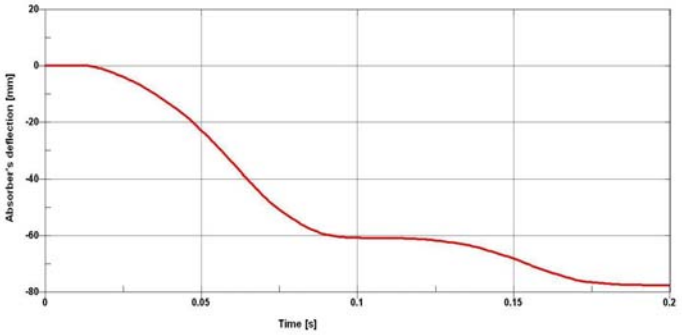

Fig. 9 change in the displacement of the shock-absorber's body against its cylinder as recorded at the touchdown

The performance of elastic-and-damping elements, by means of which the landing-gear's shock absorber has been modelled, reaches the maximum value after approximately 0.18 s simulation. This observation has been confirmed with the analysis of the plot of the displacement of the shock-absorber's body against the cylinder's sleeve. Such the plot that illustrates changes in the displacement of the shock-absorber's body against the cylinder's sleeve has been presented in Fig. 9.

The maximum value of the displacement of the shock-absorber's body against its cylinder's sleeve, found in the course of numerical simulation of the vertical drop of the main landing gear exposed to tests, has reached the value of 82 mm. The relative difference between the compared results does not exceed, therefore, 5%.

High compatibility of numerical-analysis findings and laboratory parameters of the drop test capable of recording has been also confirmed with the, e.g. reactive force recorded upon the drop-weight plate at the stage of touchdown. The maximum value of the vertical response recorded in a statical way (under the equivalent load that corresponds to the shock-absorber deflection of 82 mm) on the laboratory test stand has attained 39.5 kN. The maximum value of the vertical response found by means of numerical simulation of the drop has exceeded 45 kN. The compared values differ, therefore, by 12%, and only.

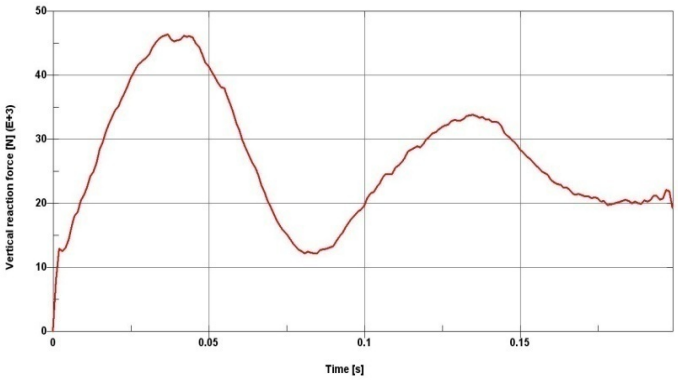

Fig. 10 change in the vertical response recorded on the model of a drop-weight plate at the touchdown

VI. FE ANALYSIS OF THE 3D LANDING GEAR MODEL WITH FAILURE

At this stage of the computer investigations given consideration, numerical tests were performed to simulate the drop of the structure with the same parameters presented in section V.

Complete 3D model of main landing gear with failure discussed above (see Fig. 1, 5) was used in dynamic analysis. In this 3D deformable model with failure developed in drop test simulation (Fig. 8 a, b) the following matters were taken into consideration: contact problems between collaborating elements and surfaces of fractures, the phenomena of energy absorption by gas-liquid damper placed in the landing gear and the response of the landing gear during touchdown of a flexible wheel with the ground.

The effects of these computations with LS-Dyna code [6] are showed in Fig. 11, 12 and 13.

The maximum principal stresses in the area of welded joint that connects the upper and lower levers of the main landing gear where the crack gap developed during drop test simulation with 3D model with 50% of the discontinuity has reached 1470 MPa (Fig. 13) and the maximal strains in the notch area [23] about 3,5% (Fig. 12).

Results gained from the simulation have proved that 3D numerical model of complete landing gear with failure is very useful. Problem of contact between mating components and surfaces of fractures, investigation into kinematics of the landing gear, and investigation into the problem of dissipation (change) of energy in the whole system and the checking of possible failure influence on the structure behaviour, which can appear in some elements due to overload can be taken into consideration here.

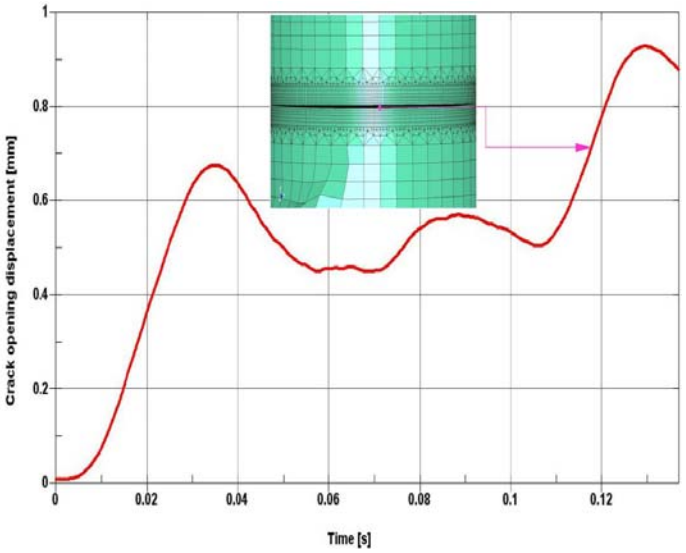

Fig. 11 change in the crack opening displacement recorded on the numerical model of main landing gear with failure in the area of welded joint that connects the upper and lower levers (see Fig. 8 a, b)

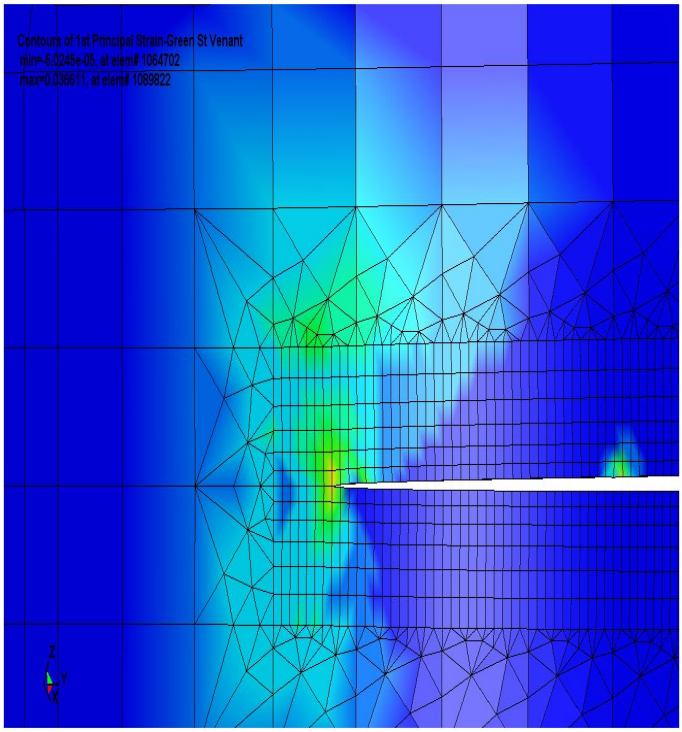

Fig. 12 map of principal strain in the area of welded joint that connects the upper and lower levers of the main landing gear where the crack gap developed during drop test simulation (see Fig. 1). The maximal strains in the notch area about 3,5%.

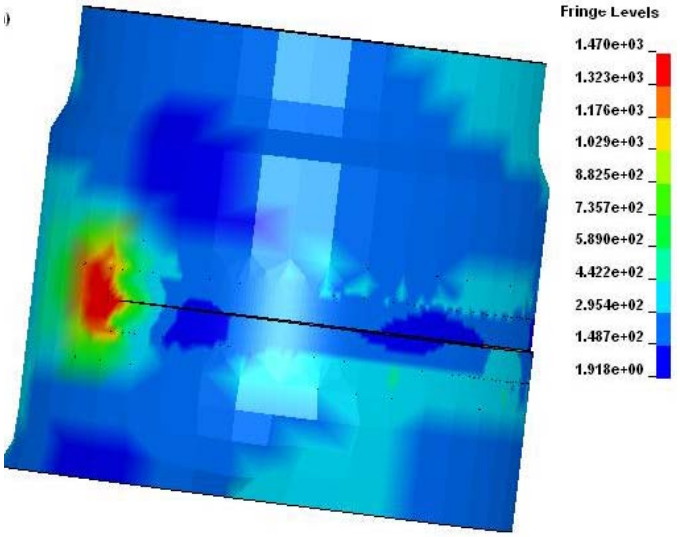

Fig. 13 map of maximum principal stresses in the area of welded joint that connects the upper and lower levers of the main landing gear where the crack gap developed during drop test simulation (see Fig. 1) (σ_{max} = 1470 MPa)

VII. Conclusion

Results of numerical analyses for some selected drop tests and results from experiments carried out on a real landing gear confirm high quality of results gained from the dynamic simulation in the model of a complete landing-gear configuration.

Results of numerical analyses on how to represent different tests performed on a drop-weight testing machine were used to generate a landing-gear model; operation-induced failures/damages to the system under consideration would be included. Results gained from the simulation have proved how effective the 3D numerical model is and how many problems can be solved in the course of only one numerical run, e.g. the geometric and material non-linearities, the question of contact between mating components, investigation into kinematics of the landing gear, and investigation into the problem of dissipation (change) of energy in the whole system and the checking of possible failure influence on the structure behaviour, which can appear in some elements due to overload.

The major advantage of the presented numerical method is applicability thereof to landing gear testing with artificially introduced flaws, what is impossible to be performed with other methods, including experimental testing work. This might include investigation into conditions hazardous to the operation of the landing gear. Furthermore, the method enables optimisation of values of some selected physical quantities of the landing-gear.

References

[1] A. G. Bagdasaryan, "Mathematical and computer tools of discrete dynamic modeling and analysis of complex systems in control loop", *International Journal Of Mathematical Models And Methods In Applied Sciences*, Issue 1, Volume 2, 2008.

[2] A Airoldi., G Janszen., "A design solution for a crashworthy landing gear with a new triggering mechanism for the plastic collapse of metallic tubes," *Aerospace Sc. and Tech* 9, 2005, pp. 445-455.

[3] W. Blajer, *Numeryczne modelowanie czasoprzestrzenne dynamicznych zagadnień kontaktowych*, IPPT PAN, 1997, (in polish).

[4] FAR–23: *Airworthiness Standards, Normal, Utility, Acrobatic and Commuter Category Airplanes*, 1966.

[5] T. Fukashima, H. Shimonishi, K. Hayashi, M. Shiraishi, *Simulation of a vehicle running on to a curb by using tire and vehicle FE Models*, 4th European LS-Dyna Users conference, Detroid, 1998.

[6] J.O. Hallquist, *LS-Dyna. Theoretical manual*. California Livermore Software Technology Corporation, 2005.

[7] H.C. Lee, Y.H. Hwang, T. Kim., "Failure analysis of nose landing gear assembly", *Engineering Failure Analysis*, vol.10, 2003, pp.77-84.

[8] M.P. Kaplan , T. A. Wolff, *Damage tolerance assessment of CASA, landing gear*. Willis & Kaplan, Inc, 2002.

[9] P.D. Khapane, "Simulation of asymmetric and typical ground maneuvers for large transport aircraft", *Aerospace Sc. and Tech.* 7, 2003, pp. 611-619.

[10] D.P. Lockard, M.R. Khorrami, *Aeroacoustic analysis of a simplified landing gear*. The Proc. of 10th AIAA/CEAS, 2003.

[11] J. Malachowski, W. Krason, A. Budzynski, "Numerical investigations of shimmy vibrations in transport aircraft's landing gear", *NiT-Nauka, Innowacje, Technika*, 3/2005 (10), pp. 38-43.

[12] W. Krason, J. Malachowski, *Dynamics analysis of the main landing gear in 3d model*, Journal of KONES Powertrain and Transport', Vol. 14, /No. 3, 2007, pp. 305-310.

[13] J.I. Pritchard, *An overview of landing gear dynamics*, NASA/TM-1999-209143, ARL-TR-1976, 1999.

[14] M. Shiraishi, K. Hayashi, N. Iwasaki, *Making FEM tire model and applying it for durability simulation*. 6th International LS-Dyna Users conference, Detroid, 2000

[15] C. Timbrell, R. Chandwani, *Residual stress in 3D Finite Element fracture mechanics analysis.* FENET Technology Workshop – Durability and Life extension, Palma Majorca, March 25-26, 2004.

[16] O.C. Zienkiewicz, *The Finite Element Method*, McGraw –Hill, New York, 1977.

[17] C. R. Azvedo, E. Hippert, "Fracture of aircraft's landing gear", *Enginiering Failure Analysis*, Vol. 9, 2002, pp. 265-275.

[18] L. A. L. Franco, N. J. Lourenco, M. L. A. Graca, O. M. M. Silva, P. P. Campos, C. F. A. "Dollinger, Fatigue fracture of a nose landing gear in a military transport aircraft", *Engineering Failure Analysis*, Vol. 13, 2006, pp. 474-479.

[19] E. A. Ossa, "Failure analysis of civil aircraft landing gear", *Engineering Failure Analysis*, Vol. 13, 2006, pp. 1177-1183.

[20] V. A. Trofimov, A. G. Molyar, "Some reasons for fracture of load-bearing elements of landing gears made of high-strength steels in Antonov airplanes", *Material Science*, Vol. 38, No. 3, 2002, pp.445-448.

[21] Ke-ge Liu, Chu-liang Yan, Shu-ming Zhang, "Estimation of fatigue damage of airplane landing gear", *Front. Mech. Eng.* 4, China, 2006, pp. 424−428.

[22] E. Ehsan Maani Miandoab, A. Yousefi-Koma, D. Ehyaei, "Optimal Design of an Impact Damper for a Nonlinear Friction-Driven Oscillator", *International Journal Of Mathematical Models And Methods In Applied Sciences*, Issue 1, Volume 2, 2008.

[23] S.R. Sabbagh-Yazdi, N.E. Mastorakis, M. Esmaili, "Explicit 2D Matrix Free Galerkin Finite Volume Solution of Plane Strain Structural Problems on Triangular Meshes", *International Journal Of Mathematics And Computers In Simulation*, Issue 1, Volume 2, 2008.